

*Full Paper*

## **Electrochemical-Sensor Behavior for Determination of Low Urea Concentration using Graphite-TiO<sub>2</sub> Composites Immobilized in a Glass Tube**

**Dwipayogo Wibowo,<sup>1,\*</sup> Wa Ode Suci Indah Sari,<sup>2</sup> Anwar Said,<sup>3</sup> Faizal Mustapa,<sup>4</sup> Bernadetha Susianti,<sup>5</sup> Maulidiyah Maulidiyah,<sup>2</sup> and Muhammad Nurdin<sup>2</sup>**

<sup>1</sup>*Department of Environmental Engineering, Faculty of Engineering, Universitas Muhammadiyah Kendari, Kendari 93117 – Southeast Sulawesi, Indonesia*

<sup>2</sup>*Department of Chemistry, Faculty of Mathematics and Natural Sciences, Universitas Halu Oleo, Kendari 93231 – Southeast Sulawesi, Indonesia*

<sup>3</sup>*Fishery Products Technology, Faculty of Fisheries and Marine Science, Universitas Muhammadiyah Kendari, Kendari 93117 – Southeast Sulawesi, Indonesia*

<sup>4</sup>*Doctoral student of Agriculture, Department of Water Resources, Universitas Halu Oleo, Kendari 93231 – Southeast Sulawesi, Indonesia*

<sup>5</sup>*PT. Jara Silica, Sugihwaras, Jenu, Tuban 62352, East Java – Indonesia*

\*Corresponding Author, Tel.: +62853-4012-2344

E-Mail: [dwipayogo@umkendari.ac.id](mailto:dwipayogo@umkendari.ac.id)

*Received: 18 January 2022 / Received in revised form: 7 March 2022*

*Accepted: 8 March 2022 / Published online: 30 April 2022*

---

**Abstract-** A high urea compound in human blood is indicated for kidney disease, urinary tract stones, and even bladder tumors. It is necessary to take several preventive measures, starting with detecting the urea compound. This study presents the preparation of a working electrode based on graphite-TiO<sub>2</sub> (G/TiO<sub>2</sub>) composites immobilized into a glass tube for sensing urea compound under an electrochemical system. The G/TiO<sub>2</sub> composites were successfully synthesized through a physical mixing method and then immobilized into a glass tube for fabricating a working electrode to sense the urea compound under the cyclic voltammetry (CV) technique. The material characterization results show that the nano-TiO<sub>2</sub> powder is composed of irregular polycrystalline and amorphous, revealing a broad pattern with low intensity. However, the effect of amorphous materials on the expansion of the nano-sized XRD TiO<sub>2</sub>

pattern is negligible. In addition, the morphological analysis of graphite has a very tight layer of flakes with a smooth and uniform surface. At the same time, the G/TiO<sub>2</sub> composites are also granule-shaped that attached to the graphite surface, identified to cover part of the graphite surface. Under the electrochemical performance test, the excellent composition of TiO<sub>2</sub> modifier is 0.5 g mixed into graphite to sense urea compound by using CV technique under a scan rate of 0.5 V.s<sup>-1</sup> with 0.1M K<sub>3</sub>[Fe(CN)<sub>6</sub>] (+0.1M NaNO<sub>3</sub>) electrolyte solution. We obtain a standard deviation of 0.361403514 and a detection limit of 0.005976905 mg.L<sup>-1</sup> with RSDr and PRSDr values of 5.51% and 3.13%, respectively. The performance of the electrodes over 25 days showed a significant effect on stability over 10 days.

**Keywords-** Sensor; Urea; Electrode; Material; Diseases

---

## 1. INTRODUCTION

The human body's metabolic process always produces residual substances that need to be excreted, such as liquids (sweat and urine), solids (feces), and gas (farts and belching) [1,2]. Chemically, it contains several organic/inorganic chemical components, i.e., carbon dioxide (CO<sub>2</sub>), water (H<sub>2</sub>O), ammonia (NH<sub>3</sub>), urea ((NH<sub>2</sub>)<sub>2</sub>CO), sodium chloride (NaCl), etc. that should be excreted the human body to stay healthy and free from various kinds diseases [3,4]. Specifically, the liquids waste substances in the human perspiration is a residual liquid substances released by the sweat glands with the main chemical contents as inorganic (NaCl, Na<sub>2</sub>HPO<sub>4</sub>, and NaH<sub>2</sub>PO<sub>4</sub>) and organic (*L*-histidine, lactic acid, and urea) [5,6]. Meanwhile, the urine substance contains several dissolved compounds such as ((NH<sub>2</sub>)<sub>2</sub>CO), H<sub>2</sub>O, ionic substances, and organic matter [7]. These metabolic waste products are released from the human body because it is no longer helpful for the body and should be released because they are toxic and can cause disease.

High urea compound in human blood is indicated for kidney disease, urinary tract stones, and even bladder tumors [8,9]. Otherwise, decreased urea levels have shown severe damage to the liver system. As we know, the normal range of urea nitrogen in blood or serum is 5 to 20 mg/dl [10]. Any elevations in levels of blood urea nitrogen (BUN) and/or serum creatinine were usually indicated structural renal disease because it is caused by prerenal (cardiac decompensation, dehydration excessive, increased catabolism of protein and high-protein diet) and cause of renal (glomerulonephritis, chronic nephritis acute, diseases polycystic kidney, and tubular necrosis) and postrenal causes (all types of obstruction of the urinary tract, such as kidney stones, enlarged prostate gland, and tumors) [11]. BUN is the end product of nitrogen as a urea compound that is rapidly dispersed in the blood and excreted through the kidneys as a urine component, and a small amount of urea is excreted through sweat [12]. This impact results in kidneys failure are one of the chronic diseases in Indonesia country [13]. So, it is necessary to take several preventive measures, starting with detecting the urea levels in the blood. Nowadays, the standard method has been applied for measuring blood urea levels using the spectrophotometric method [14,15]. It can measure urea concentration in the normal range

below with a detection limit of 5 to 20 mg/dL (50 to 200 mg.L<sup>-1</sup>) [16]. However, this method was required a large number of samples and difficult for users because of the high operation tool, expensive tests, and required special skills. Therefore, a faster and high-accurate analytical method is needed to detect blood urea levels, namely the electrochemical process.

Electrochemistry provides a widely used analytical technique for detecting persistent organic pollutants due to its fast response, low cost, portability, and easy preparation [17–21]. This paper presents G/TiO<sub>2</sub> composites preparation as a working electrode for detecting urea compounds based on the electrochemical method. This method is easily applied for measuring low concentration samples because it is very sensitive to the electric current generated from the redox reaction, which is to measure low concentration samples because it is very sensitive to the electric current generated from the redox reaction, proportional to the sample concentration [22–24]. An electrochemical sensor is most suitable for sensing urea compound in blood or urine because it applies the working principle of electrochemical interactions between analytes and electrodes to become analytically useful signals [25,26]. Importantly, the electrode components are required for experimental methods for electron transfer or analyte redox reactions [27–31].

The TiO<sub>2</sub> semiconductor is an attractive material for working electrodes because of its advantages, such as high potential range, sensitivity, selectivity, inert, environmentally friendly, non-toxic, suitable for various sensors, and inexpensive [32–34]. Although, the graphite material is unstable electric current performance due to weak forces between layer planes material and the tendency of graphitic materials to fracture along planes. In this study, we present functionalized materials from graphite that serve as high-absorption of the urea and are forwarded into the TiO<sub>2</sub> semiconductor to high-response of electrochemical performance.

## 2. EXPERIMENTAL METHOD

### 2.1. Preparation of graphite-TiO<sub>2</sub> composites

In this section, both samples are prepared as working electrode that will be applied to the voltammetric technique. First, we present a pristine graphite powder (Sigma, Aldrich, Dorset, UK) that has been crushed and sifted using 200 mesh. It was heated at 80°C to obtain a high porosity carbon material. Second, TiO<sub>2</sub>-P25 (Sigma, Aldrich, Dorset, UK) was easily prepared by sieving under 200 mesh and inserted into a porcelain dish and calcined at 500°C for 3 hours to obtain the TiO<sub>2</sub> crystal. Both samples were mixed by adding liquid paraffin (Sigma, Aldrich, Dorset, UK) as a binder, and varied the mass composition of TiO<sub>2</sub>-P25 including 0.01 g, 0.1 g, and 0.5 g. The G/TiO<sub>2</sub> composites are stirred and inserted into a glass tube as an electrode body while being pressed to solidify and rubbed until smooth, flat, and shiny.

## 2.2. Electrochemical Performance

### 2.2.1. Electrolyte test

The electrochemical test was conducted to determine the high-current response of electron transfer under 0.01 M NaNO<sub>3</sub> (Sigma, Aldrich, Dorset, UK) and 0.01 M K<sub>3</sub>[Fe(CN)<sub>6</sub>] (Sigma, Aldrich, Dorset, UK) as electrolyte solutions, then tested using a working electrode using the CV technique. This technique aims to determine the current and potential responses which is generated by the working electrode material against electrolyte solution. Experimentally, the preparation of 0.01 M NaNO<sub>3</sub> and 0.01 M K<sub>3</sub>[Fe(CN)<sub>6</sub>] electrolyte solutions was applied by weighing 0.085 g NaNO<sub>3</sub> (Mr= 85 g.mol<sup>-1</sup>) and 0.329 g K<sub>3</sub>[Fe(CN)<sub>6</sub>] (Mr = 329 g.mol<sup>-1</sup>) and dissolved by distilled water in a 100 mL volumetric flask to the lower meniscus line and homogenized. The voltammetry technique has been applied using a three-electrode system, namely G/TiO<sub>2</sub> composites as a working electrode, Ag/AgCl as a reference electrode, and Pt wire as an auxiliary electrode. They are inserted into a voltammetry cell containing an electrolyte solution and measured in the potential range from -0.8 V to 0.8 V at a scan rate of 0.5 V.s<sup>-1</sup> to observe the optimal current response.

### 2.2.2. Sensor parameters

Electrodes are inserted into voltammetry cells containing 0.05 mg.L<sup>-1</sup> urea compound [(NH<sub>2</sub>)<sub>2</sub>CO] (Sigma, Aldrich, Dorset, UK) and electrolyte solution. Optimum scan rate test measured by a variation of 0.1; 0.2; 0.5; and 0.05 V.s<sup>-1</sup> under the potential range of -0.8 V to 0.8 V. The high response of the scanning rate is applied for some further testing. The detection limit is also determined by varying the concentration of [(NH<sub>2</sub>)<sub>2</sub>CO] by 0.05; 0.1, 0.15, and 0.2 mg.L<sup>-1</sup> (+electrolyte) using CV techniques. The sample's current, potential, and concentration are plotted as linearity curves to find detection limits, where the smallest concentration still provides an analyte signal that the instrument can measure. We also tested electrode repeats by continuously measuring the best composition of the G/TiO<sub>2</sub> composites for 30 times. This treatment uses cyclic voltammetry containing 0.05 mg.L<sup>-1</sup> [(NH<sub>2</sub>)<sub>2</sub>CO]+[electrolyte] and is determined using the peak current of each measurement to determine the relative standard deviation (RSD) value of the G/TiO<sub>2</sub> composites. In addition, reproducibility performance was also determined for 25 days in the range of every three days tested electrode activity. Finally, the selectivity test of the G/TiO<sub>2</sub> composites uses 0.01, 0.05, and 0.1 mg.L<sup>-1</sup> Pb(NO<sub>3</sub>)<sub>2</sub> as an interference ion in the electrochemical system.

### 2.2.3. Characterization of G/TiO<sub>2</sub> composites

TiO<sub>2</sub> was characterized using X-Ray Diffraction (PANalytical, X'Pert PRO) to observe the crystal form of the resulting material. Morphological analysis was also determined to find material interactions between carbon and TiO<sub>2</sub>. Physical interactions of materials were monitored, such as surface and particle size, generally using a scanning electron microscope

(SEM FEI, Inspect-S50 with EDX). Then, functional groups were applied to observe the carbon bond and the presence of  $\text{TiO}_2$  material.

### 3. RESULTS AND DISCUSSION

#### 3.1. Fabrication of working electrode based on a glass tube

The working electrode body consists of copper wire, electrode tubes, and electrode materials. In particular, the copper wire is used as a conductor to transfer electrons from the material to the potentiostat. First, it is cut to a length of 5.0 cm and sanded until smooth, flat, and shiny; this is intended to current flow properly during the measurement process. After that, it is inserted into the glass tube. At the end of the electrode, it gives a little space for the electrode material to copper not come into direct contact with the electrolyte solution. The G/ $\text{TiO}_2$  material in the electrode that will be in direct contact with the electrolyte solution [35]. If the copper wire comes into direct contact with the electrolyte, it will affect the electrochemical results. G/ $\text{TiO}_2$  composites are the working electrode material prepared via physical contact with carbon, paraffin, and  $\text{TiO}_2$ . Then, it was heated at  $80^\circ\text{C}$  and allowed to stand for 24 hours to solidify and increase the contact between particles. In this case, we varied the  $\text{TiO}_2$  with three weight variations, namely 0.01, 0.1, and 0.5 g, respectively, which were put in a glass tube to apply as a working electrode.

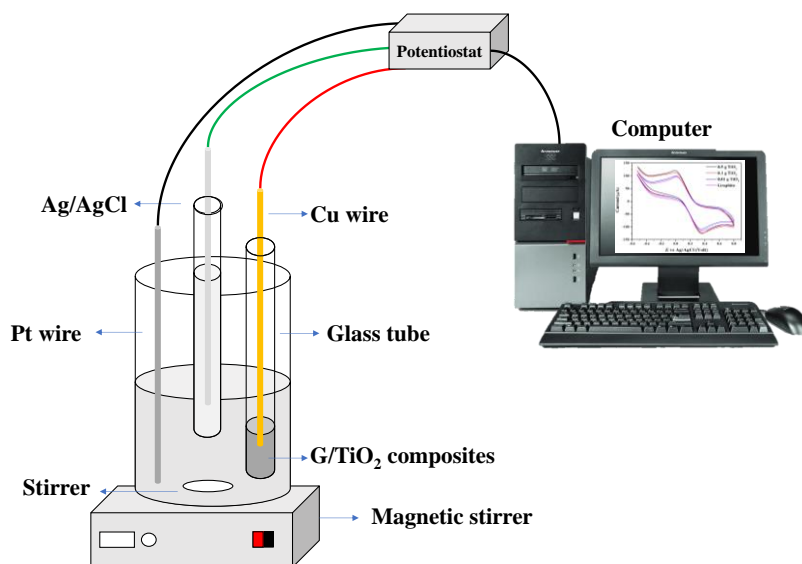


**Figure 1.** Schematic illustration of the electrochemical test using three electrodes system

#### 3.2. Material Characterizations

This section discussed the crystal form of  $\text{TiO}_2$  that has been calcined at  $500^\circ\text{C}$  for 3 hours. To elucidate the effect of  $\text{TiO}_2$  on the lattice structure of pure graphite,  $\text{TiO}_2$  was prepared via the calcination process to observe the crystal formed on the graphite surface [36]. According

to Maulidiyah et al. [37], the formation of high crystallinity in TiO<sub>2</sub> material can be activated under the calcination process at a temperature of 500°C to obtain anatase or rutile crystals. Experimentally, we observed visually that the calcined TiO<sub>2</sub> has fine aggregates and clean (white) particles. This method also aims to remove impurities mixed with TiO<sub>2</sub>. After that, it was characterized using an XRD instrument to observe the crystallinity of the materials (Figure 1).

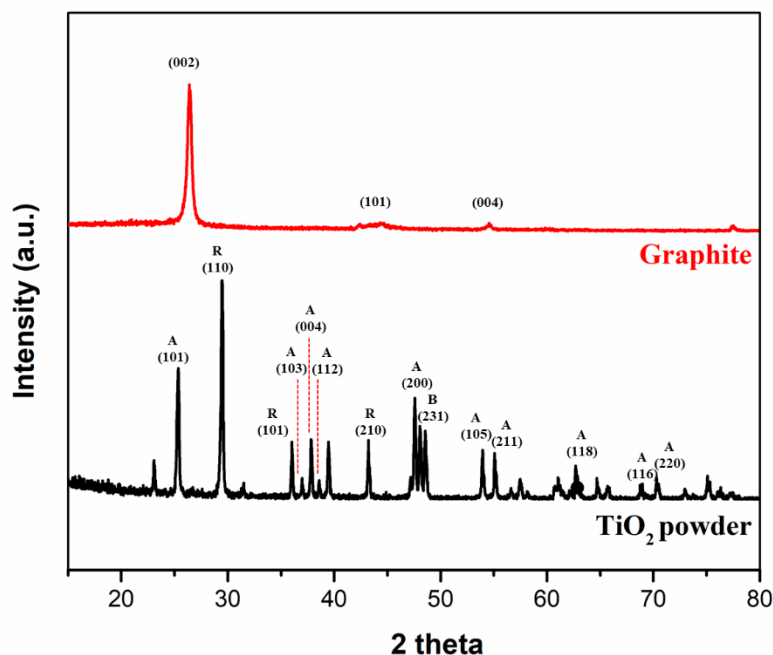


**Figure 2.** XRD pattern of graphite and TiO<sub>2</sub> powder (A=Anatase, R=Rutile, and B = Brookite)

To elucidate the TiO<sub>2</sub> crystal form in high-performance are needed several parameters, including the crystalline, atomic, and molecular structure and phase evaluation [38]. The TiO<sub>2</sub> calcinated was evaluated using the corresponding XRD pattern, shown in Fig. 2. The anatase peaks that are located at  $2\theta = 25.35^\circ$ ,  $37.01^\circ$ ,  $37.87^\circ$ ,  $38.57^\circ$ ,  $47.59^\circ$ ,  $53.95^\circ$ ,  $55.07^\circ$ ,  $62.70^\circ$ ,  $68.75^\circ$ , and  $70.29^\circ$  are assigned as (101), (103), (004), (112), (200), (105), (211), (118), (116), and (220) that has been confirmed with JCPDS No. 84-1286 and reported by [39]. In otherwise, the rutile peaks also that are detected at  $2\theta = 29.49^\circ$ ,  $36.03^\circ$ , and  $43.23^\circ$  are assigned as (110), (101), and (210), then one peak detected of brookite crystal located at  $2\theta = 48.57^\circ$  (231), respectively. The rutile and brookite have been confirmed with JCPDS No. JCPDS 88-1175 and JCPDS No. 39-1360 [39,40]. These results suggested that the nano-TiO<sub>2</sub> powder is composed of irregular polycrystalline. Amorphous revealed a broad pattern with low intensity; however, the effect of the amorphous materials on the broadening of the XRD patterns of nano-sized TiO<sub>2</sub> is negligible [39].

We also reported the results of morphological analysis on graphite and G/TiO<sub>2</sub> composites by varying magnifications of 1000 times, 5000 times, and 20,000 times. Based on Figure 3, the surface of graphite has extremely close flake layers with a smooth and uniform surface. The

physical treatment at a temperature of 80°C resulted in intercalated graphite [41]. According to [41], the expanded graphite is formed by the collapse of the parallel boards of the intercalated graphite, which deforms randomly, resulting in many pores of different sizes. In addition, they also confirm that individual graphite nanosheets are not single graphene, but consist of several layers of graphite sheets, and the surface morphology of graphite material is delicate and irregular sheets, as has already been observed in Figure 3b and Figure 3c. While the G/TiO<sub>2</sub> composites are granule-shaped and the surface is white, it is identified to cover part of the graphite surface. TiO<sub>2</sub> powder (approximately 1 μm) densely loaded on the graphite (Figure 3d, 3e, 3f) that closely combined and covered some parts with the graphite surface. The graphite and TiO<sub>2</sub> were attributed to the lattice oxygen (Ti-O) in TiO<sub>2</sub> and the surface hydroxyl group of TiO<sub>2</sub> (Ti-OH) that formed with C-O bonds [36].

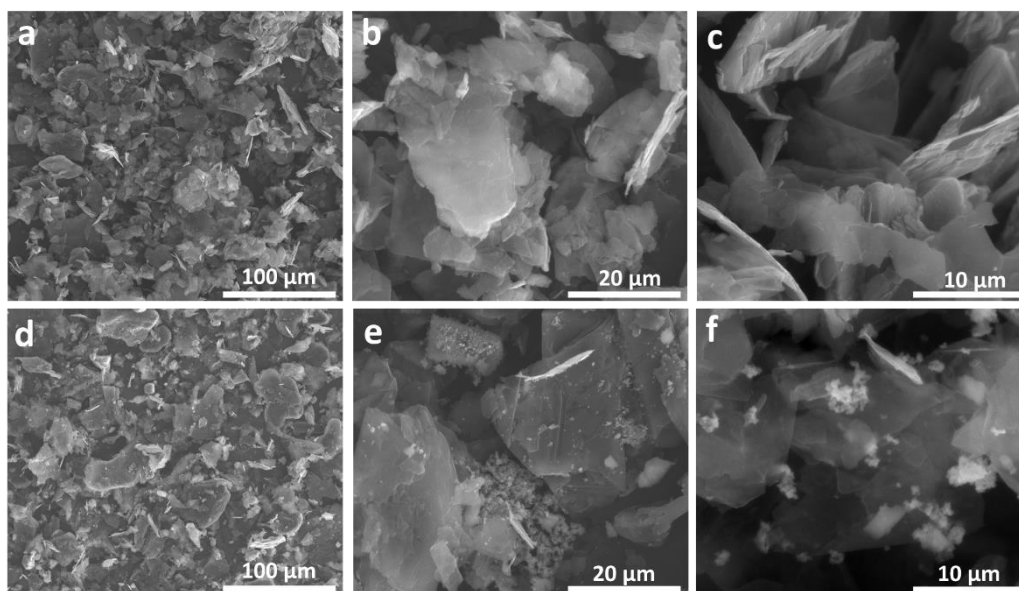


**Figure 3.** Image of graphite (**a**: 1000 times, **b**: 5000 times, and **c**: 20000 times) and G/TiO<sub>2</sub> composites (**d**: 1000 times, **e**: 5000 times, and **f**: 20000 times)

EDX spectra data of graphite and G/TiO<sub>2</sub> composites were measured at a voltage of 15 kV. The spectrum is a characteristic X-ray captured by a Si detector. The graphite EDX Figure 4a shows that the carbon atoms (C) and oxygen atoms (O) have the quantities captured by each detector at 0.15 and 0.25 KeV. The significant atomic intensity of C is due to the graphite structure consisting of the bonds of the carbon atoms. However, the graphite is not pure, which is only suspended over carbon atmos, since it still finds Si element appear probably due to the chamber effect of SEM-EDX [42]. For G/TiO<sub>2</sub>, the Titanium atoms (Ti) have been detected at 4.5 and 4.9 KeV, and still finds Ca and Si elements appear probably due to the chamber effect of SEM-EDX and TiO<sub>2</sub> isolated from the mineral sand.

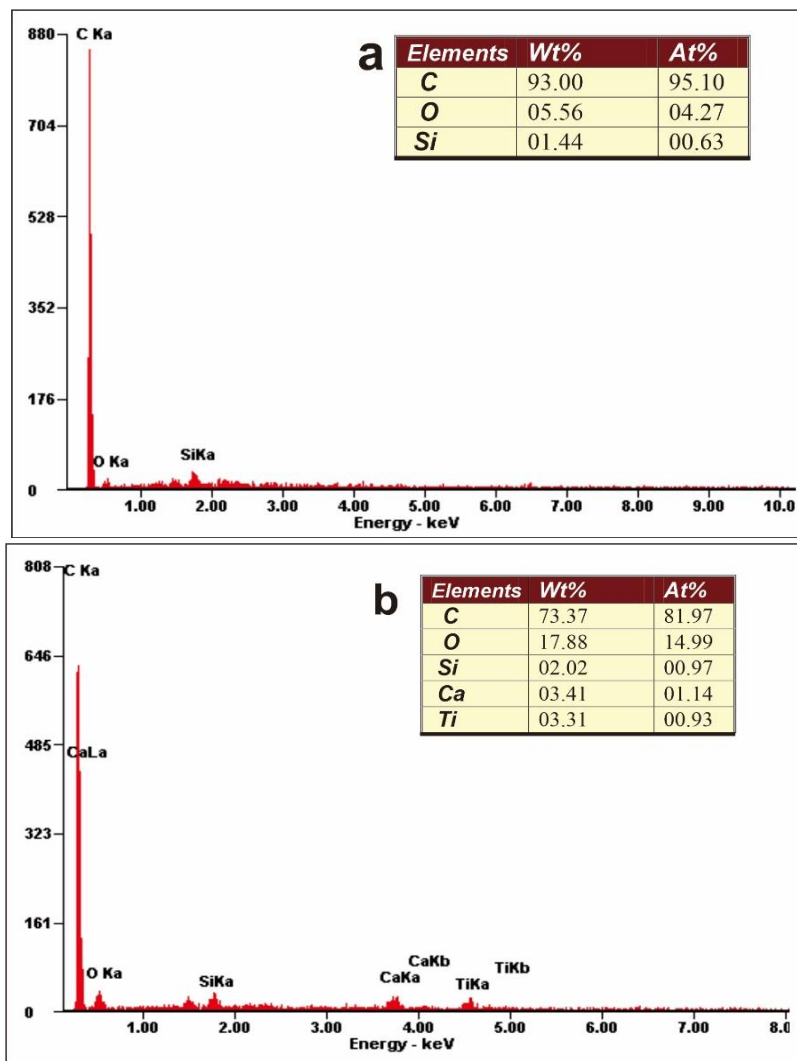


**Figure 4.** EDX spectra; (a) graphite and (b) G/TiO<sub>2</sub> composites

### 3.3. Electrochemical Performance

#### 3.3.1. Electrolyte Test

For the electrolyte test, we applied the G/TiO<sub>2</sub> composites mobilized into a glass tube under electrolyte solutions K<sub>3</sub>[Fe(CN)<sub>6</sub>] and NaNO<sub>3</sub> with CV technique. In addition, electrolyte variations aim to compare the performance of electrodes produced against current responses from peak values  $I_{pa}$  (current anodic) and  $E_{pa}$  (potential anodic) and as good stability for electron transfer in the system. The electrolyte tests were examined with three electrodes system, namely Ag/AgCl as the reference electrode, platinum wire as the auxiliary electrode, and working electrode based on G/TiO<sub>2</sub> composites mobilized into a glass tube. It was put into each solution of 0.1M K<sub>3</sub>[Fe(CN)<sub>6</sub>], 0.1 M NaNO<sub>3</sub>, and 0.1M K<sub>3</sub>[Fe(CN)<sub>6</sub>] (+0.1M NaNO<sub>3</sub>).

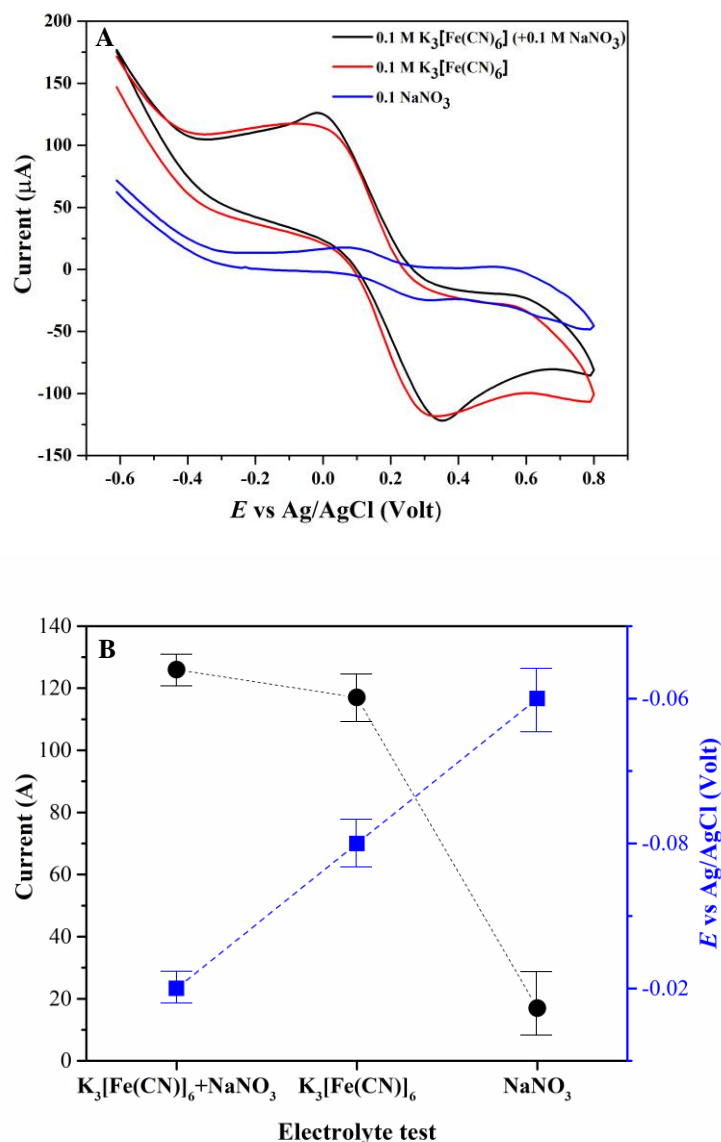


**Figure 5.** Voltammogram of G/TiO<sub>2</sub> composites; (A) CV curve with the difference of electrolyte solution, and (B) The  $I_{pa}$  and  $E_{pa}$  values based on the difference of electrolyte solution

Based on the results show (Figure 5A) that 0.1M  $K_3[Fe(CN)_6]$  (+0.1M  $NaNO_3$ ) has produced the highest current response with an  $I_{pa}$  value of 126  $\mu A$ . It is due to reversible electrochemical behavior and an easy electron transfer in the system. Then, the  $K_3[Fe(CN)_6]$  is an electroactive oxidizing agent capable of capture electrons well with a standard potential value of 0.35 V [43]. The role of  $NaNO_3$  electrolyte serves as a conductor of electric current in the solution so that the analyte is not affected by the difference in potential changes that are given quickly [44,45]. It is a suitable electrolyte that will be used in subsequent analyses. Fig. 5B exhibits the  $I_{pa}$  and  $E_{pa}$  values based on Fig. 5A, the oxidation and reduction responses based on the peak of high current and potential from each electrolyte. The excellent

performance using  $\text{K}_3[\text{Fe}(\text{CN})_6]$  (+0.1M  $\text{NaNO}_3$ ) electrolyte against working electrode which characterized by the high current response and low error. It is due to the reversible redox reactions in the voltammetric cell according to the following equation (1):

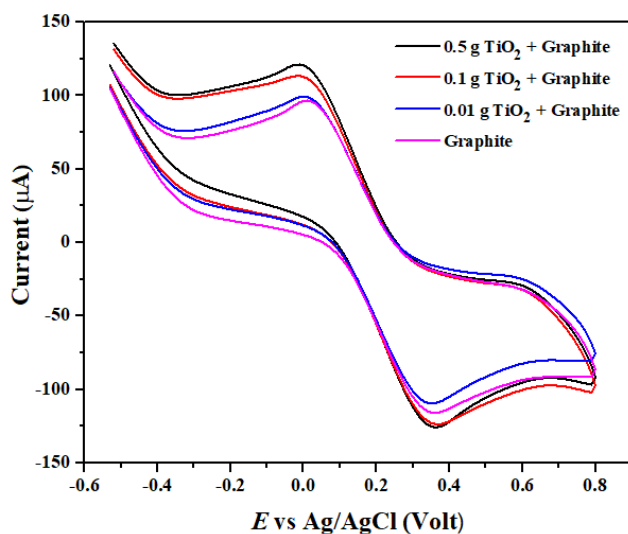


A comparison of anodic and cathodic peak currents states that the reactions in the  $\text{Fe}(\text{CN})_6^{3-}/\text{Fe}(\text{CN})_6^{4-}$  system are reversible [46].

### 3.3.2. Sensor Performance Test

#### 3.3.2.1. Mass optimization of $\text{TiO}_2$ modifier in graphite material

The mass variation effect was examined against the  $\text{TiO}_2$  modifier mixed into the graphite material and tested by the CV technique. It can provide information on the redox reactions of organic compounds from the electron movement of currents. In addition, the electrode that gives the highest peak current value and is close to the reversible reaction is selected as the best electrode. Anodic and cathodic peaks indicate the number of electrochemical reaction steps and are indicators of reaction reversibility [47]. Determination of mass optimization of  $\text{TiO}_2$  modifier was carried out by testing each G/ $\text{TiO}_2$  composites as a working electrode made in several mass variations of modifier, namely 0.01 g, 0.1 g, 0.5 g, and without  $\text{TiO}_2$ . Each electrode was immersed in a voltammetric cell containing 0.1M  $\text{K}_3[\text{Fe}(\text{CN})_6]$  electrolyte solution (+0.1M  $\text{NaNO}_3$ ). After obtaining a good mass optimization of the  $\text{TiO}_2$  modifier in graphite, it was used for further analysis based on the validity of the sensor, such as linearity, repeatability, selectivity, sensitivity, and detection limit. The results of the measurement of the mass variation of the  $\text{TiO}_2$  modifier are shown in Figure 6.



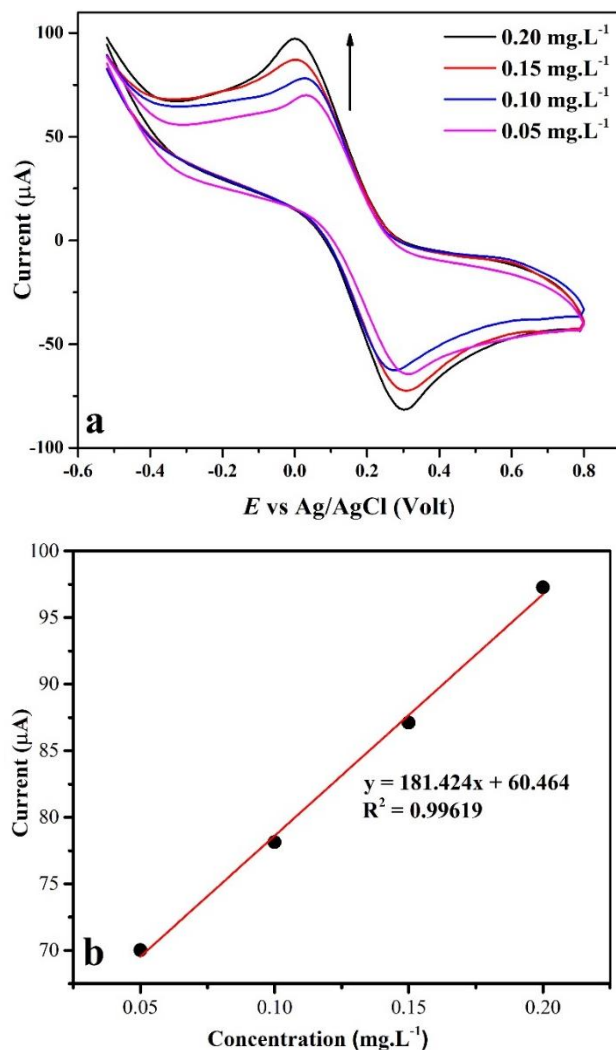
**Figure 6.** Voltammogram with added and without the addition of  $\text{TiO}_2$  modifier

Figure 6 shows the voltammogram results measured by a scan rate of  $0.5 \text{ V}\cdot\text{s}^{-1}$  under a potential range of  $-0.8 \text{ V}$  to  $0.8 \text{ V}$ . The peak current formed on the voltammogram represents the periodic movement of electrons from the chemical reaction on the electrode surface. The mass ratio of G/TiO<sub>2</sub> affects the current produced, where each electrode gives a different current response. The highest peak current value of  $I_{\text{pa}}$  is generated with the mass of the TiO<sub>2</sub> modifier with 0.5 g of  $I_{\text{pa}}$  value of  $121 \mu\text{A}$  and the  $E_{\text{pa}}$  value of  $-0.01 \text{ V}$ . The increasingly large mass of the TiO<sub>2</sub> modifier will generate the highest peak value of  $I_{\text{pa}}$  caused by the presence of TiO<sub>2</sub> as semiconductor material that contributes to high electron transfer by inducing electron signals. The electrons in TiO<sub>2</sub> will move from the valence band to the conduction band resulting in high electron movement, while graphite's role as an electron stabilizer is for the electron transfer rate to run well [48–50]. The working electrode was fabricated with 0.5 g of TiO<sub>2</sub> modifier as an excellent electrode for generating a higher current response than another mass.

### 3.3.2.2. Determination of detection limit

In this section, a linearity test was examined to identify the characteristics of a sensor to represent the size of the sample quantity range. The high concentration is proportional to the high current response to observe the range of sample concentrations between the signals generated by the potentiostat instrument against sample concentration. The relationship between current response with sample concentration has an impact on the current response. It is the basis for determining the value of the detection limit for analytical measurements. Experimentally, the urea compound as a sample is determined by measuring the concentration of 0.05; 0.10; 0.15, and 0.2  $\text{mg}\cdot\text{L}^{-1}$  in  $\text{K}_3[\text{Fe}(\text{CN})_6]$  electrolyte. Determination of linearity area and detection limit of urea compound was carried out using scan rate  $0.5 \text{ V}\cdot\text{s}^{-1}$  with a potential range from  $-0.8 \text{ V}$  to  $0.8 \text{ V}$ , and the measurement results are made a calibration curve of the relationship between urea concentration on the X-axis and  $I_{\text{pa}}$  value on the Y-axis as shown in Figure 7.

Figure 7 is the result of a linearity curve, where Figure 7a is a cyclic voltammogram with a difference in sample concentration. The increase of current response is proportional to the increase of samples concentration, while Figure 7b is the  $I_{\text{pa}}$  value plotted against the concentration. The data showed that the linearity equation had been obtained with a slope value of 181.424 and an intercept of 60.464, with a linear regression value of  $R^2 = 0.99619$ , categorized as a linearity area approaching 0.999 or 1. Linearity also describes the sensitivity of the working electrode, expressed from the slope value of the graph. If the response is linear, the sensitivity will also be the same for the entire measurement range. Figure 7b is used as reference data to determine the detection limit to calculate the standard deviation. Based on the experiment results, we obtained a standard deviation value of 0.361403514 and a detection limit value of  $0.005976905 \text{ mg}\cdot\text{L}^{-1}$ . This suggests that G/TiO<sub>2</sub> electrode has good detection capabilities for urea compound with high sensitivity.



**Figure 7.** Linearity curve, (a) Cyclic voltammogram with concentrations variation and (b)  $I_{pa}$  value versus concentrations

### 3.3.2.3. Repeatability and Reproducibility tests

In general, both tests were characterized as precision tests with time differences. The repeatability test is a precision test to determine the degree of conformity between the results of the electrode test with the average value obtained in repetition at one time, while. In contrast, the reproducibility test is a precision test at on some days. Experimentally, these tests were applied to observe the working electrode stability in a urea solution of  $0.05 \text{ mg. L}^{-1}$  30 times, while the reproduction test is examined every 3 days checked for 25 days which aims to find out the optimum period of G/TiO<sub>2</sub> composites that is still feasible in the determination of urea. The measurement results can be seen in Figure 8.

Based on Figure 8, repeatability and reproducibility tests showed that the working electrode experienced decreased performance with time-increase variation due to saturation on the surface and oxidation reactions in the material. The repeatability test of the G/TiO<sub>2</sub> electrode (Figure 8a and Figure 8b) can be determined by calculating the standard deviation (SD) and

relative standard deviation (RSD) based on the peak flow result of  $0.05 \text{ mg.L}^{-1}$  urea so that we obtained an SD value of 4.54 and the average current of  $85.53 \mu\text{A}$  with RSDr and PRSDr values of 5.51% and 3.13%, respectively. The repeatability test is well stated if the HorRat ratio is less than 2 [51–53]. Based on the results of calculations, the G/TiO<sub>2</sub> electrode is declared stable. On the other hand, the reproducibility test also experienced a decrease in performance within a few days. Figure 8c and Figure 8d can be seen that the optimum stability electrode performance was shown at 10 days based on the current value data generated above  $80.507 \mu\text{A}$ . The continuous electrode used can cause a thickening of the diffusion layer on the working electrode surface, resulting in slower electron transfer and a decrease in peak current [54].

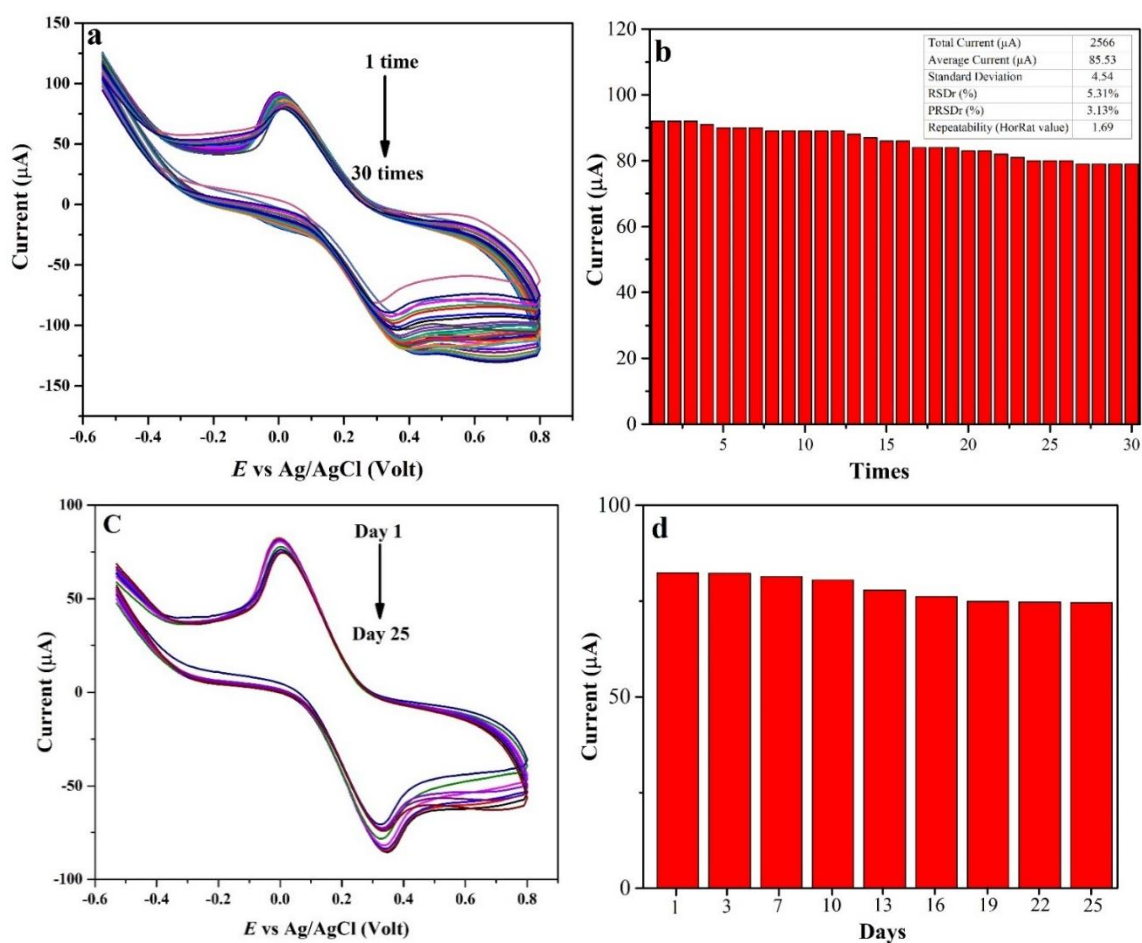


**Figure 8.** Repeatability and Reproducibility tests; (a) Voltammogram of repeatability, (b) Repeatability graph, (c) Voltammogram of reproducibility, (d) Reproducibility graph

#### 3.3.2.4. Interference ions test

We also tested the addition of interference ions  $\text{Pb}(\text{NO}_3)_2$  ( $0.01$ ,  $0.05$ , and  $0.1 \text{ mg.L}^{-1}$ ) into the electrochemical system to observe the selectivity of specific ions in the solution and assess the potentiometry sensor due to the presence of interference ions will affect the analytic signals recorded by the instrument. In solution,  $\text{Pb}(\text{NO}_3)_2$  will decompose into  $\text{Pb}^{2+}$  and  $\text{NO}_3^{2-}$  ions

which will destabilize the  $\text{NH}_3$  of the urea compound decomposed by aqueous solutions. The selected  $\text{Pb}(\text{NO}_3)_2$  as a disrupting compound because it is abundant in the air, soil, and water, leading to the development of more widespread pollution transmission to the human body. This compound will eventually enter the blood and will be excreted through urine. Figure 9 shows that the presence of interference ions in the system can affect the measurement results, along with the increase in the concentration of  $\text{Pb}(\text{NO}_3)_2$  indicating a low  $I_{\text{pa}}$  value due to the presence of interfering ions attached to the electrode surface, the number of sample ions at the electrode decreases, the diffusion layer thickens to slow electron transfer and saturation on the electrode surface.

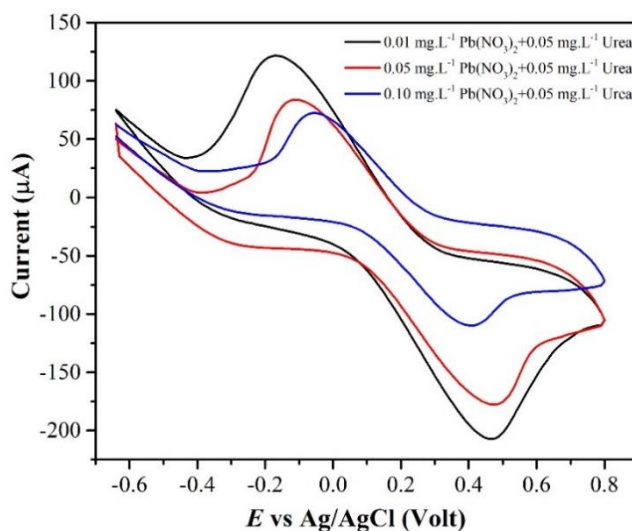


**Figure 9.** Voltamogram of the effect of  $\text{Pb}(\text{NO}_3)_2$  in urea compound

#### 4. CONCLUSION

We conclude that the graphite mixed in  $\text{TiO}_2$  powder as a working electrode material has been achieved via the physical mixing under an environmentally friendly technique. The nano- $\text{TiO}_2$  powder is composed of irregular polycrystalline, and amorphous, revealing a broad pattern with low intensity. In addition, morphology analysis of graphite has shown the very tight layer of flakes with a smooth and uniform surface. At the same time, the G/ $\text{TiO}_2$  composites are granule-shaped, the surface is white and identified to cover part of the graphite surface. The electrochemical performance shows the  $\text{TiO}_2$  modifier is 0.5 g mixed into graphite for use as a working electrode to detect urea compounds under scan rate  $0.5 \text{ Vs}^{-1}$  with 0.1M  $\text{K}_3[\text{Fe}(\text{CN})_6]$  (+0.1M  $\text{NaNO}_3$ ) electrolyte solution. The experiment obtained a standard deviation value of 0.361403514 and a detection limit value of 0.005976905 mg.L<sup>-1</sup> with RSDr and PRSDr values of 5.51% and 3.13%, respectively. The performance of the electrodes over 25 days showed a significant effect on stability over 10 days.

## Acknowledgments

We acknowledge the Muhammadiyah Batch V Research Grant of 2021 No. 0842.100/PD/I.3/C/2021 under financial support and Titania Research Group-Universitas Halu Oleo to implement this research.

## Declarations of interest

The authors declare that there are no conflicts of interest in this article.

## REFERENCES

- [1] V. Maksimova, N. Shalginskikh, O. Vlasova, O. Usalka, A. Beizer, P. Bugaeva, D. Fedorov, O. Lizogub, E. Lesovaya, and R. Katz, *PLoS One* 16 (2021) e0252504.
- [2] J. L. Bormann, A. S. Filiz Acipayam, and H. I. Maibach, *J. Appl. Toxicol.* 41 (2021) 194.
- [3] H. W. Smith, *The kidney: structure and function in health and disease*, Oxford University Press (1951).
- [4] D. Cianciosi, T. Y. Forbes-Hernández, S. Afrin, M. Gasparrini, P. Reboredo-Rodriguez, P. P. Manna, J. Zhang, L. Bravo Lamas, S. Martínez Flórez, and P. Agudo Toyos, *Molecules* 23 (2018) 2322.
- [5] H. He, H. Zeng, Y. Fu, W. Han, Y. Dai, L. Xing, Y. Zhang, and X. Xue, *J. Mater. Chem. C* 6 (2018) 9624.
- [6] J. Li, X. Yang, Z. Zhang, H. Xiao, W. Sun, W. Huang, Y. Li, C. Chen, and Y. Sun, *J. Hazard. Mater.* 403 (2021) 123614.
- [7] T. Zhou, Y. Feng, T. Thomas-Danguin, and M. Zhao, *Food Chem.* 335 (2021) 127664.
- [8] P. Stenvinkel, J. Painer, M. Kuro-o, M. Lanasa, W. Arnold, T. Ruf, P. G. Shiels, and R. J. Johnson, *Nat. Rev. Nephrol.* 14 (2018) 265.
- [9] C. C. Chen, J. C. Hsieh, C. H. Chao, W. S. Yang, H. T. Cheng, C. K. Chan, C. J. Lu, H. F. Meng, and H. W. Zan, *J. Breath Res.* 14 (2020) 036002.
- [10] H. K. Walker, W. D. Hall, and J. W. Hurst, *Clinical Methods*, 3rd edition, Boston: Butterworths (1990).
- [11] N. Baum, C. C. Dichoso, and C. E. Carlton, *Urology* 5 (1975) 583.
- [12] A. F. Schranck, *Analysis of Electrochemical Systems for Decomposition of Urea in urine*, University of Notre Dame (2019).
- [13] A. Y. Arifiyanto, A. D. Laksono, D. Chalidyanto, N. Tantiasari, and W. Kusumaningtyas, *Indian J. Forensic Med. Toxicol.* 15 (2021) 1867.
- [14] Z. Aghamiri, M. Safaei, and M. R. Shishehbor, *J. Chinese Chem. Soc.* 68 (2021) 95.
- [15] V. M. Nurchi, R. Cappai, N. Spano, and G. Sanna, *Molecules* 26 (2021) 3071.
- [16] A. Tricoli, and G. Neri, *Sensors* 18 (2018) 942.
- [17] T. Azis, M. Maulidiyah, M. Z. Muzakkar, R. Ratna, S. W. Aziza, C. M. Bijang, O. A. Prabowo, D. Wibowo, and M. Nurdin, *Surf. Eng. Appl. Electrochem.* 57 (2021) 387.

- [18] H. Karimi-Maleh, F. Karimi, L. Fu, A. L. Sanati, M. Alizadeh, C. Karaman, and Y. Orooji, *J. Hazard. Mater.* 423 (2022) 127058.
- [19] H. Karimi-Maleh, Y. Orooji, F. Karimi, M. Alizadeh, M. Baghayeri, J. Rouhi, S. Tajik, H. Beitollahi, S. Agarwal, and V. K. Gupta, *Biosens. Bioelectron.* 184 (2021) 113252.
- [20] H. Medetalibeyoğlu, M. Beytur, S. Manap, C. Karaman, F. Kardaş, O. Akyıldırım, G. Kotan, H. Yüksek, N. Atar, and M. L. Yola, *ECS J. Solid State Sci. Technol.* 9 (2020) 101006.
- [21] C. Karaman, O. Karaman, B. B. Yola, İ. Ulker, N. Atar, and M. L. Yola, *New J. Chem.* 45 (2021) 11222.
- [22] D. Wibowo, Y. Sufandy, I. Irwan, T. Azis, M. Maulidiyah, and M. Nurdin, *J. Mater. Sci. Mater. Electron.* 28 (2020) 14375.
- [23] M. Nurdin, L. Agus, A. A. M. Putra, M. Maulidiyah, Z. Arham, D. Wibowo, M. Z. Muzakkar, and A. A. Umar, *J. Phys. Chem. Solids* 131 (2019) 104.
- [24] M. Nurdin, N. Dali, I. Irwan, M. Maulidiyah, Z. Arham, R. Ruslan, B. Hamzah, S. Sarjuna, and D. Wibowo, *Anal. Bioanal. Electrochem.* 10 (2018) 1538.
- [25] A. Singh, A. Sharma, A. Ahmed, A. K. Sundramoorthy, H. Furukawa, S. Arya, and A. Khosla, *Biosensors* 11 (2021) 336.
- [26] M. Maulidiyah, I. B. P. Wijawan, D. Wibowo, A. Aladin, B. Hamzah, and M. Nurdin, *IOP Conf. Ser. Mater. Sci. Eng.* 367 (2018) 012060.
- [27] Hikmawati, A. H. Watoni, D. Wibowo, Maulidiyah, and M. Nurdin, *IOP Conf. Ser. Mater. Sci. Eng.* 267 (2017) 012005.
- [28] A. A. Ensafi, and H. Karimi-Maleh, *Electroanalysis* 22 (2010) 2558.
- [29] M. A. Khalilzadeh, H. Karimi-Maleh, A. Amiri, and F. Gholami, *Chinese Chem. Lett.* 21 (2010) 1467.
- [30] S. N. Azizi, S. Ghasemi, and S. Kaviani, *Biosens. Bioelectron.* 62 (2014) 1.
- [31] J. B. Raof, R. Ojani, and H. Karimi-Maleh, *J. Appl. Electrochem.* 39 (2009) 1169.
- [32] M. Maulidiyah, P. E. Susilowati, N. K. Mudhafar, Z. Arham, and M. Nurdin, *Biointer. Res. App. Chem.* 12 (2021) 1628.
- [33] D. Wibowo, M. Z. Muzakkar, M. Maulidiyah, M. Nurdin, S. K. M. Saad, and A. A. Umar, *Biointerface Research in Applied Chem.* 12 (2021) 1421.
- [34] M. Natsir, Y. I. Putri, D. Wibowo, M. Maulidiyah, L. O. A. Salim, T. Azis, C. M. Bijang, F. Mustapa, I. Irwan, Z. Arham, and M. Nurdin, *J. Inorg. Organomet. Polym. Mater.* 31 (2021) 3378.
- [35] E. G. Shim, T. H. Nam, J. G. Kim, H. S. Kim, and S. I. Moon, *Electrochim. Acta* 54 (2009) 2276.
- [36] W. Zhang, M. Gao, F. Miao, X. Wu, S. Wang, and X. Wang, *J. Hazard. Mater.* 418 (2021) 126318.

- [37] Maulidiyah, M. Nurdin, Erasmus, D. Wibowo, M. Natsir, H. Ritonga, and A. H. Watoni, *Int. J. Chem.Tech. Res.* 8 (2015) 645.
- [38] F. Khojasteh, M. R. Mersagh, and H. Hashemipour, *J. Alloys Compd.* 890 (2022) 161709.
- [39] K. Thamaphat, P. Limsuwan, and B. Ngotawornchai, *Kasetsart J.* 42 (2008) 357.
- [40] Y. Wang, L. Li, X. Huang, Q. Li, and G. Li, *RSC Adv.* 5 (2015) 34302.
- [41] L. S. Montagna, F. D. C. Fim, G. B. Galland, and N. R. D. S. Basso, *Macromol. Symp.* 299–300 (2011) 48.
- [42] R. Siburian, H. Sihotang, S. Lumban Raja, M. Supeno, and C. Simanjuntak, *Orient. J. Chem.* 34 (2018) 182.
- [43] C. Kalinke, N. V. Neumsteir, P. R. de Oliveira, B. C. Janegitz, and J. A. Bonacin, *Anal. Chim. Acta* 1142 (2021) 135.
- [44] D. Wibowo, Maulidiyah, Ruslan, T. Azis, and M. Nurdin, *Anal. Bioanal. Electrochem.* 10 (2018) 465.
- [45] M. Z. Muzakkar, A. A. Umar, I. Ilham, Z. Saputra, and L. Zulfikar, *J. Phys. Conf. Ser.* 1242 (2019) 1.
- [46] R. G. Compton, J. C. Eklund, and S. D. Page, *J. Phys. Chem.* 99 (1995) 4211.
- [47] M. Nurdin, O. A. Prabowo, Z. Arham, D. Wibowo, M. Maulidiyah, S. K. M. Saad, and A. A. Umar, *Surfaces and Interfaces* 16 (2019) 108.
- [48] Nurhidayani, M. Z. Muzakkar, Maulidiyah, D. Wibowo, and M. Nurdin, *IOP Conf. Ser. Mater. Sci. Eng.* 267 (2017) 12035.
- [49] M. Maulidiyah, D. Wibowo, H. Herlin, M. L. Andarini, Ruslan, and M. Nurdin, *Asian J. Chem.* 29 (2017) 2504.
- [50] D. Wibowo, M. Z. Muzakkar, S. K. M. Saad, F. Mustapa, M. Maulidiyah, M. Nurdin, and A. A. Umar, *J. Photochem. Photobiol. A* 398 (2020) 112589.
- [51] N. Belkhamza, L. Ouattara, and M. Ksibi, *J. Electrochem. Soc.* 162 (2015) B212.
- [52] W. Horwitz and R. Albert, *J. AOAC Int.* 89 (2006) 1095.
- [53] M. Nurdin, O. A. Prabowo, Z. Arham, D. Wibowo, M. Maulidiyah, S. K. M. Saad, and A. A. Umar, *Surfaces and Interfaces* 16 (2019) 108.
- [54] K. G. Lim, and G. T. R. Palmore, *Biosens. Bioelectron.* 22 (2007) 941.